RSC Advances

COMMUNICATION

View Article Online
View Journal | View Issue

CrossMark click for updates

Cite this: *RSC Adv.*, 2015, **5**, 25777

Received 6th January 2015
Accepted 5th March 2015

DOI: 10.1039/c5ra03585f

www.rsc.org/advances

Open Access Article. Published on 05 2015. Downloaded on 18/12/2025 10:09:25 .
This article is licensed under a Creative Commons Attribution 3.0 Unported Licence.

Mesoporous poly(ethylene-*co*-vinyl alcohol) monolith captured with silver nanoparticles as a SERS substrate: facile fabrication and ultra-high sensitivity†

Guowei Wang,[a] Hiroyuki Yoshikawa,[b] Eiichi Tamiya[b] and Hiroshi Uyama*[a]

A facile method to fabricate a mesoporous poly(ethylene-*co*-vinyl alcohol) (EVOH) monolith captured with silver nanoparticles (AgNPs) was developed. The formation of AgNPs and the monolith was in a one-pot process. The obtained monolith demonstrated ultrasensitive surface-enhanced Raman spectroscopy (SERS) responses.

SERS has attracted the interest of scientists as a powerful technique to detect chemical and biological molecules of trace concentration. The ultra-high sensitivity is due to the enhancement of the local electromagnetic field caused by nano-scale gaps (also called Raman "hot spots") between metal nanostructures. Metal nanoparticles or nanostructures in types of roughed metal electrodes,[1–3] metal nanoparticles colloids,[4–6] metal nanoparticles-assembled planar substrates[7,8] and metal nanoparticles-embedded three-dimensional (3-D) porous substrates[9] have been developed as efficient SERS substrates. Among these SERS substrates, the 3-D porous ones are preferred because the open pores and the high surface area enable fast permeation and efficient adsorption of target analytes, respectively. In addition, the porous structure is considered to be able to improve the SERS performance on a large scale.[10]

So far, various 3-D porous SERS substrates have been prepared by immobilizing metal nanoparticles into a porous matrix such as porous gel,[10] nanofiber,[11] porous alumina,[9] porous silicon,[12] monolith,[13,14] MOF[15] and paper.[16] For the construction of SERS substrates, a facile, cost-effective and largely-scalable method is highly demanded. However, the preparation of metal nanoparticles and a porous matrix is generally in separated processes, which is costly and somewhat wearisome. Thus, it remains a great challenge for preparation of 3-D porous SERS substrates by a simply one-pot process.

Polymer monoliths with mesoporous structure have been developed in our group by a facile thermally induced phase separation (TIPS) method.[17,18] Mesoporous polymer monoliths with open pores and large surface areas are especially useful for applications of 3-D porous SERS substrates. In order to get monolith-based 3-D SERS substrates with uniform mesopores, well dispersed metal nanoparticles and high SERS signal reproducibility, facile synthesis of a metal–polymer monolith using a one-pot process is indispensable and of particular interest.

In this study, we report a new and straightforward method to embed AgNPs into a mesoporous EVOH monolith (AgNPs–EVOH monolith). A simple one-pot process yielded AgNPs–EVOH monolith with uniform mesopores and well dispersed AgNPs. We further demonstrated that the monolith could be used as a SERS substrate with both ultrasensitive SERS responses and high SERS signal reproducibility. Our study enables the preparation of a 3-D porous SERS substrate with a facile method, which is as simple as other methods.[19,20]

The general procedure for the fabrication of the mesoporous AgNPs–EVOH monolith is illustrated in Fig. 1. Silver nitrate was added to an EVOH solution of a mixed solvent of isopropanol (IPA) and water (IPA/water: 65/35 (v/v)) at 75 °C and the solution was gently stirred. The solution was cooled to 4 °C to form a monolith by TIPS. The resulting monolith was immersed into acetone to remove the embedded solvent and subsequently

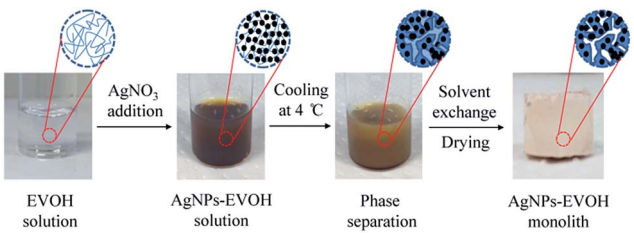

Fig. 1 A general procedure for fabrication of AgNPs–EVOH monolith.

[a]Department of Applied Chemistry, Graduate School of Engineering, Osaka University, Suita 565-0871, Japan. E-mail: uyama@chem.eng.osaka-u.ac.jp; Fax: +81-6-6879-7367; Tel: +81-6-6879-7364

[b]Department of Applied Physics, Graduate School of Engineering, Osaka University, Suita 565-0871, Japan. Fax: +81-6-6879-7840; Tel: +81-6-6879-7839

† Electronic supplementary information (ESI) available. See DOI: 10.1039/c5ra03585f

Open Access Article. Published on 05 2015. Downloaded on 18/12/2025 10:09:25 .
This article is licensed under a Creative Commons Attribution 3.0 Unported Licence.

dried under vacuum. In this method, IPA acted both as a component of the mixed solvent to dissolve EVOH at the high temperature and as an agent for the reduction of the silver ion; the analysis of the solution after the monolith formation suggested that more than 97% of silver ion was reduced. EVOH was initially acted as a stabilizer to protect AgNPs from large scale aggregation and subsequently acted as a gelator to form the monolith with uniform mesopores. The present simple method to prepare the metal nanoparticles-embedded monolith is suitable for large scale production. Moreover, the monolith could be tailored into any desired shapes for the further SERS applications.

The nitrogen adsorption/desorption isotherms of the monolith exhibited a typical V isotherm with a relatively wide type H1 hysteresis loop in the P/P_0 range from 0.7–0.9, which is the characteristic of the mesoporous structure (Fig. 2). The formation of uniform mesopores centred at *ca.* 5.0 nm was proved by the pore size distribution (PSD) plot (insert), which was obtained by using the non-local density functional theory (NLDFT) method. The specific surface area was determined as 60.1 m^2 g^{-1} by multi-point BET method. These data indicate that the AgNPs–EVOH monolith had relative uniform mesopores and large specific surface area.

Fig. 3A shows a scanning electron microscope (SEM) image of the monolith. The SEM image clearly indicates the 3-D open macropore structure of the monolith. The existence of both mesopores and macropores enabled the capture of more target analysts and faster transport of these molecules to the surface of AgNPs. A transmission electron microscopy (TEM) image implies the existence of AgNPs with a typical diameter of 5–20 nm (Fig. 3B). It is interesting that most of the formed AgNPs were not spatially-isolated, but partially aggregated as silver dimers or clusters (Fig. S1†). Many researchers revealed that strong SERS signals often present at the junction of several nanoparticles.[21] On the other hand, single nanoparticles often result in little enhancement. Thus, the formation of partially aggregated AgNPs made the monolith a potential SERS substrate with ultra sensitivity. The corresponding energy dispersive X-ray spectrometric (EDX) map (Fig. 3C) of the monolith shows that the AgNPs were dispersed homogeneously in the 3-D porous monolith, although the EDX mapping was somewhat affected by the rough surface of the monolith. Fig. 3D demonstrates the SERS spectrum of rhodamine 6G (R6G) from the monolith that was treated with a R6G solution at concentration of 10^{-6} M. R6G showed characteristic SERS peaks, whereas the monolith exhibited clear background without any significant peaks in the Raman shift range from 900 cm^{-1} to 1900 cm^{-1}. All of these results indicate that the present monolith could be used as a good SERS substrate.

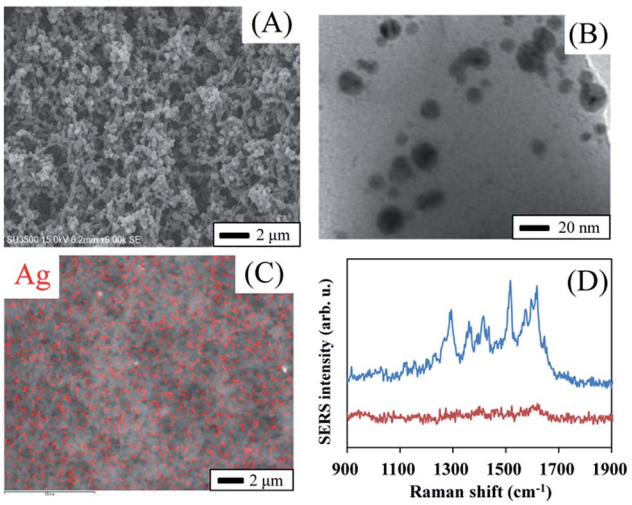

Fig. 3 SEM (A), TEM (B) and EDX (C) (red spots represent the existence of AgNPs) images of AgNPs–EVOH monolith. SERS spectrum (—) of R6G collected from the monolith and Raman spectrum (—) of the monolith (without R6G) (D).

To evaluate the efficiency of the AgNPs–EVOH monolith as a SERS substrate, 4-mercaptobenzoic acid (MBA) was selected as a target analyte. We immersed the monolith into 10 mL of ethanol solution containing 10^{-5} M of MBA for 2 h. After post-treatment of the monolith (Fig. S2†), the SERS spectrum of the monolith was measured by using the equipment as showed in Fig. S3.† SERS spectra of MBA collected from 10 randomly selected positions of the monolith are shown in Fig. 4. A peak

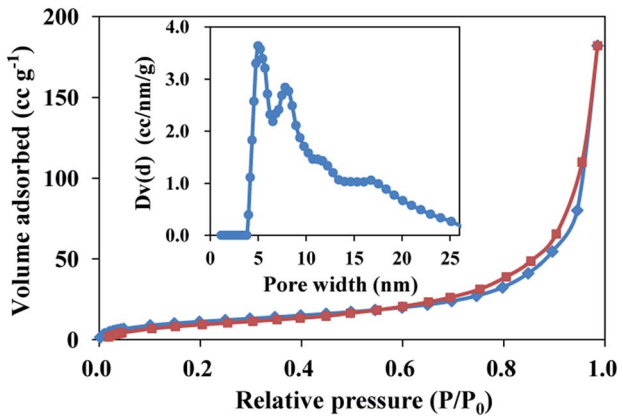

Fig. 2 Nitrogen adsorption/desorption isotherms of AgNPs–EVOH monolith. Adsorption points are marked by blue tetragons and desorption points by dark red tetragons.

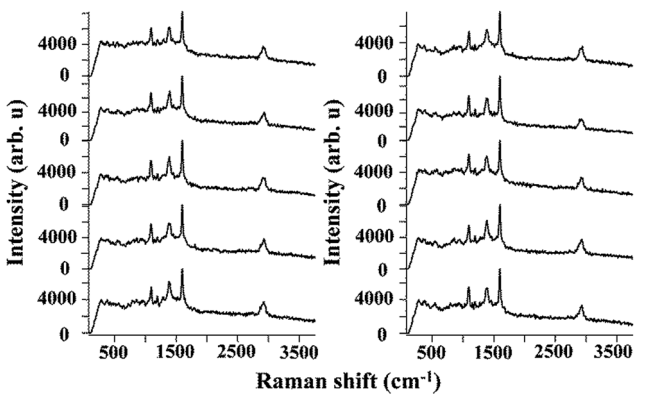

Fig. 4 Series of SERS spectra measured in the randomly selected 10 places on the AgNPs–EVOH monoliths.

This journal is © The Royal Society of Chemistry 2015

Open Access Article. Published on 05 2015. Downloaded on 18/12/2025 10:09:25 .
This article is licensed under a Creative Commons Attribution 3.0 Unported Licence.

at around 1390 cm^{-1} arose from carboxyl stretching mode and peaks observed at around 1100 cm^{-1} and 1600 cm^{-1} could be attributed to breathing and stretching modes of aromatic ring, respectively.[22] It should be noted that the SERS responses of the monolith showed good consistency and reproducibility, which is vital in consideration of its practical applications. This may be due to the good dispersion of AgNPs in the monolith.

Several monoliths with different amount of silver nitrate were prepared in order to investigate the influence of the AgNPs concentration. The SEM images (Fig. S4†) clearly show that the monoliths had similar continuous open pores when the weight ratio of silver nitrate/EVOH was equal or lower than 0.67, whereas the monoliths were in non-porous structure in case of the ratio of larger than 0.67. This may be because the IPA/water ratio is changed owing to the consumption of IPA in the Ag^{+} reduction process. The SERS spectra of MBA were collected on these samples. Even for the low concentration of MBA (10^{-11} M), the porous monolith showed clear SERS spectra with the same peak positions and similar intensity (Fig. S5a–c†), whereas no clear spectra were obtained in case of the non-porous monolith (Fig. S5d and e†). These data indicate that the AgNPs concentration hardly affected the Raman enhancement, while the porous structure was vitally important. Some researchers also revealed the large effect of porous structure in Raman enhancement.[10] Additionally, the intensity ratio of the peak at 1600 cm^{-1} and the peak at 2500 cm^{-1}, which represents the MBA peak intensity normalized by the background intensity, was examined (Fig. S6†). The intensity ratio at even very low MBA concentration was much larger than that of the monolith without MBA, strongly suggesting that the present monolith has ultra-high sensitivity toward MBA.

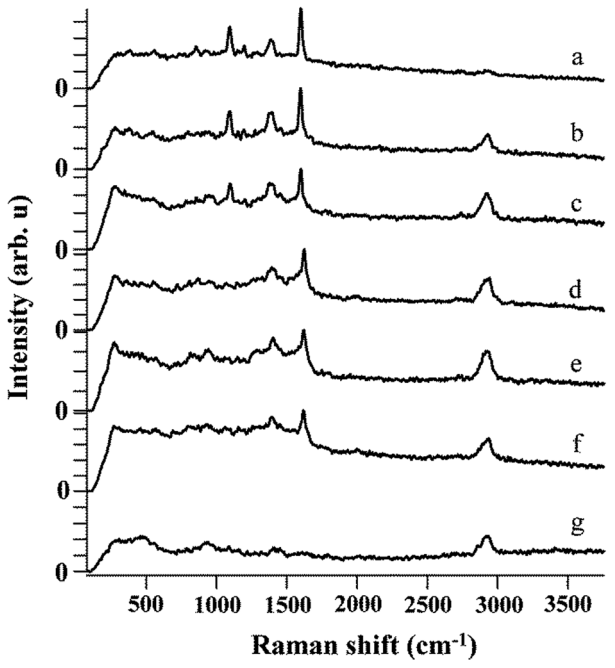

Fig. 5 SERS spectrum of MBA on SERS substrate with concentrations of (a) 10^{-3} M, (b) 10^{-5} M, (c) 10^{-7} M, (d) 10^{-9} M, (e) 10^{-11} M, (f) 10^{-13} M, (g) 0 M.

The SERS sensitivity of the monolith toward MBA was investigated by immersing the monolith in the ethanol solution with a wide range of the MBA concentrations from 10^{-3} M to 10^{-13} M. The characteristic Raman peaks of MBA were clear when the MBA concentration was equal or higher than 10^{-7} M (Fig. 5). Even the MBA concentration was as low as 10^{-13} M, the peaks at 1100 cm^{-1} and 1600 cm^{-1} were still identifiable, indicating that the present monolith could be applied for ultrasensitive detection of target analysts. Compared with some other SERS substrates, the present monolith showed better sensitivity toward MBA.[23,24]

In this communication, a unique method was developed for the generation of the AgNPs embedded mesoporous monolith. The monolith with uniformly dispersed AgNPs exhibited both ultrasensitive SERS responses and high Raman signal reproducibility toward MBA. Compared with conventional 3-D porous SERS substrates, which need complicated fabrication process, the proposed method enabled facile one-pot fabrication of the porous material. We believe that the present 3-D porous SERS substrate has great potential for *in situ* chemical or biological studies.

Acknowledgements

This study is financially supported by a Grant-in-Aid for Scientific Research from the Japan Society for the Promotion of Science (no. 25288090) and a Project for Creating Start-ups from Advanced Research and Technology, MEXT.

Notes and references

1 B. Ren, X. F. Lin, J. W. Yan, B. W. Mao and Z. Q. Tian, *J. Phys. Chem. B*, 2003, **107**, 899–902.
2 P. Gao, D. Gosztola, L. W. H. Leung and M. J. Weaver, *J. Electroanal. Chem.*, 1987, **233**, 211–222.
3 P. Gao and M. J. Weaver, *J. Phys. Chem.*, 1985, **89**, 5040–5046.
4 J. Zhang, X. Li, X. Sun and Y. Li, *J. Phys. Chem. B*, 2005, **109**, 12544–12548.
5 M. Muniz-Miranda, M. Pagliai, G. Cardini and V. Schettino, *J. Phys. Chem. C*, 2008, **112**, 762–767.
6 B. Pergolese, A. Bonifacio and A. Bigotto, *Phys. Chem. Chem. Phys.*, 2005, **7**, 3610–3613.
7 F. Toderas, M. Baia, L. Baia and S. Astilean, *Nanotechnology*, 2007, **18**, 255702.
8 O. Seitz, M. M. Chehimi, E. Cabet-Deliry, S. Truong, N. Felidj, C. Perruchot, S. J. Greaves and J. F. Watts, *Colloids Surf., A*, 2003, **218**, 225–239.
9 H. Ko, S. Chang and V. V. Tsukruk, *ACS Nano*, 2009, **3**, 181–188.
10 S. Yao, C. Zhou and D. Chen, *Chem. Commun.*, 2013, **49**, 6409–6411.
11 Y. Qian, G. Meng, Q. Huang, C. Zhu, Z. Huang, K. Sun and B. Chen, *Nanoscale*, 2014, **6**, 4781–4788.
12 A. Virga, P. Rivolo, E. Descrovi, A. Chiolerio, G. Digregorio, F. Frascella, M. Soster, F. Bussolino, S. Marchiò,

Open Access Article. Published on 05 2015. Downloaded on 18/12/2025 10:09:25 .
This article is licensed under a Creative Commons Attribution 3.0 Unported Licence.

F. Geobaldo and F. Giorgis, *J. Raman Spectrosc.*, 2012, **43**, 730–736.
13 J. Liu, I. White and D. L. DeVoe, *Anal. Chem.*, 2011, **83**, 2119–2124.
14 M. Guerrouache, S. Mahouche-Chergui, M. M. Chehimi and B. Carbonnier, *Chem. Commun.*, 2012, **48**, 7486–7488.
15 Y. Hu, J. Liao, D. Wang and G. Li, *Anal. Chem.*, 2014, **86**, 3955–3963.
16 Y. H. Ngo, D. Li, G. P. Simon and G. Garnier, *Langmuir*, 2012, **28**, 8782–8790.
17 K. Okada, M. Nandi, J. Maruyama, T. Oka, T. Tsujimoto, K. Kondoh and H. Uyama, *Chem. Commun.*, 2011, **47**, 7422–7424.
18 Y. Xin, T. Fujimoto and H. Uyama, *Polymer*, 2012, **53**, 2847–2853.
19 A. Lee, S. Dubinsky, E. Tumarkin, M. Moulin, A. A. Beharry and E. Kumacheva, *Adv. Funct. Mater.*, 2011, **21**, 1959–1969.
20 S. Chang, Z. A. Combs, M. K. Gupta, R. Davis and V. V. Tsukruk, *ACS Appl. Mater. Interfaces*, 2010, **2**, 3333–3339.
21 H. Xu, E. J. Bjerneld, M. Käll and L. Börjesson, *Phys. Rev. Lett.*, 1999, **83**, 4357–4360.
22 P. Xu, N. H. Mack, S. H. Jeon, S. K. Doom, X. Han and H. L. Wang, *Langmuir*, 2010, **26**, 8882–8886.
23 A. Amarjargal, L. D. Tijing, H. K. Shon, C. H. Park and C. S. Kim, *Appl. Surf. Sci.*, 2014, **308**, 396–401.
24 S. Zhu, C. Fan, J. Wang, J. He, E. Liang and M. Chao, *J. Colloid Interface Sci.*, 2015, **438**, 116–121.

This journal is © The Royal Society of Chemistry 2015